

Resonances Characteristics of Parallel Plate Waveguide Cavities

Lin Chen, Dan-Ni Wang, Yi-Ming Zhu, and Yan Peng

Abstract—The influence of air gaps on the response of transmission for a transverse-electric mode parallel-plate waveguide (TE-PPWG) with a single cavity and double cavities has been studied experimentally. As the air gap is larger than the resonant wavelength of high order cavity mode in the single deep grooved waveguide, only the fundamental cavity mode can be excited and single resonance can be observed in the transmission spectrum. Based on above observations, a tunable multiband terahertz (THz) notch filter has been proposed and the variation of air gap has turned out to be an effective method to select the band number. Experimental data and simulated results verify this band number tunability. This mechanical control mechanism for electromagnetic induced transparency (EIT) will open a door to design the tunable THz devices.

Index Terms—Electromagnetic induced transparency, metal parallel plate waveguide, terahertz filter.

1. Introduction

The parallel-plate waveguide (PPWG) is a simple structure in the THz range which is well understood in classical waveguide theory and is widely employed due to its low loss and low dispersion characteristics^[1]. Owing to the fact that waveguides have the ability to confine

radiation, they can be employed in conjunction with resonant structures, resulting in unique spectral resonant features, which opens up PPWG to a myriad of sensing and filtering applications. There have been several designs that employed resonant structures embedded within PPWGs such as Bragg gratings, photonic band gap, and resonant groove(s) structures^{[2]-[10]}. Recently, a single rectangular cavity incorporated into a transverse-electric mode PPWG (TE-PPWG) has been demonstrated as a notch filter with a very narrow line width^[11]. The PPWG with a single cavity has also been found to be a strong and high Q resonant system in which the electromagnetic induced transparency (EIT) phenomenon will appear. Astley *et al.* has characterized the single cavity waveguide resonant structure and also analyzed the origin of the resonant behavior and its dependence on geometric factors^[12]. As the groove grows deeper (i.e. depth increases), this dip shifts to lower frequencies. However, there are still some key aspects of the single grooved TE-PPWG performance that has not been sufficiently studied. It should be noted that the grooved PPWG structures are analogous to plasmonic stub metal-insulator-metal (MIM) structures in the visible region^{[13]-[16]}. The stub structure also plays an important role in filtering proposals but lacks the experimental support. Then we reported an observation of an EIT-like phenomenon in THz PPWG double cavities systems and analyzed the relation between the off-position of the cavities and the transmission properties. We also found that two detuned resonances could be varied by choosing different shifting length between double cavities. This means that the phase shift of the propagating wave between two resonances may be another important factor for the realization of EIT. The proposed system has the following features: First, since the most popular metals are seen as perfect conductors due to their extremely large conductivity in the THz region, the realization of THz EIT-like response in PPWG-cavities systems is not plasmonically induced. Second, the double cavities have identical geometry, therefore, the detuning of resonant frequencies does not arise from the different geometrical parameters of two cavities. We also found the EIT-like transmission presented here resulted from the resonances hybridization induced by the change of coupling strength of the top and bottom cavities^[17].

Manuscript received June 5, 2015; revised June 17, 2015. This work was supported by the National Program on Key Basic Research Project of China under Grant No. 2014CB339806, Basic Research Key Project under Grant No. 12JC1407100, Major National Development Project of Scientific Instrument and Equipment under Grant No. 2011YQ150021 and No. 2012YQ14000504, and the National Natural Science Foundation of China under Grant No. 11174207, No. 61138001, No. 61205094, and No. 61307126.

Y.-M. Zhu and Y. Peng are with the Shanghai Key Lab of Modern Optical System, Engineering Research Center of Optical Instrument and System, Ministry of Education, University of Shanghai for Science and Technology, Shanghai 200093, China (Corresponding authors e-mail: ymzhu@usst.edu.cn; py@usst.edu.cn)

L. Chen and D.-N. Wang are with the Shanghai Key Lab of Modern Optical System, Engineering Research Center of Optical Instrument and System, Ministry of Education, University of Shanghai for Science and Technology, Shanghai 200093, China (e-mail: linchen@usst.edu.cn; danniwang07@163.com)

Digital Object Identifier: 10.3969/j.issn.1674-862X.2015.02.007

The PPWG is a potential EIT device. This realization has encouraged a continuous research for mimicking EIT in classical systems. In the field of optics, waveguide based EIT-like resonances have been proposed numerically in resonant cavity systems. Importantly, the phase coupling between the resonators has been proved to be a key factor for EIT-like response^{[18],[19]}. This paper mainly discusses the resonances characteristics of parallel plate waveguides with a single cavity and double cavities.

2. PPWG with Single Cavity

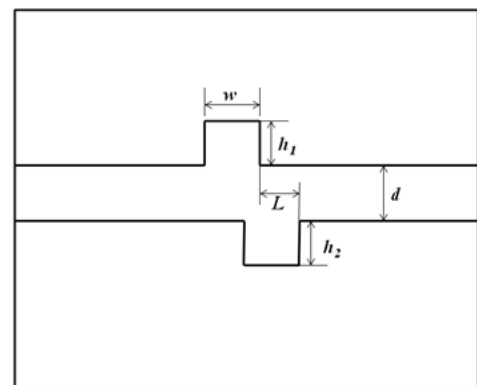
A PPWG system with a single deep cavity is shown in Fig. 1 (a), the cavity geometry is designed with a width of w and a depth of h_2 (when $h_1=0\ \mu\text{m}$, $L=0\ \mu\text{m}$), d represents the waveguide spacing between the two plates. The fundamental TE mode was excited at the beginning of the waveguide and the transmission was defined as the transmitted power through PPWG cavity structure divided by the transmitted power through PPWG without the cavity structure. We used a groove with a fixed width of $w=400\ \mu\text{m}$ based on a previous experiment^{[8],[20]}, and set the depth to be $h_2=1400\ \mu\text{m}$ as our default number. For the excitation of TE mode, the incident THz wave was applied with polarization parallelly to the plates^{[8],[20]}. The photo of PPWG with a single deep cavity is shown in Fig. 1 (b). It is formed by micro-machining a rectangular groove into bottom plates of PPWG, respectively. Each plate is made of polished nickel-plating Cu. In the experiment, we used the terahertz time domain spectroscopy (THz-TDS) system to obtain the output power spectra of PPWG with a deep cavity^{[8],[10]}. Most of these devices were measured by a high performance THz-TDS^{[21]-[25]}, which is also made by the University of Shanghai for Science and Technology, as shown in Fig. 1 (c). In this system, we used a P-I-N diode as the terahertz emitter, whose frequency can reach 4.2 THz and the scan speed reaches 10 scan/s.

Fig. 2 shows the measured time domain waveforms of free space and the grooved PPWG with $h_1=0\ \mu\text{m}$, $h_2=1400\ \mu\text{m}$, and $d=555\ \mu\text{m}$, respectively. The experimental setup has the frequency resolution of 4.58 GHz corresponding to the time domain waveforms of $\sim 218.4\ \text{ps}$.

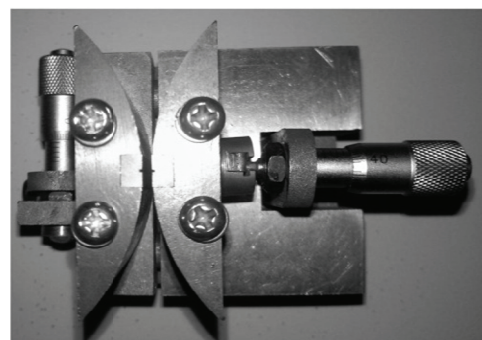
Fig. 3 shows the normalized power transmission spectra for the waveguide of three typical plate spacing with a deep groove incorporated. The spectra show the characteristics single, double, and triple resonant features for $d=800\ \mu\text{m}$, $710\ \mu\text{m}$, and $555\ \mu\text{m}$, respectively.

Fig. 4 compares the power transmission spectra of the single deep cavity PPWG with different air gaps. Power transmission spectra are calculated by using the amplitude ratio of the waveguide with and without the incorporated cavity. The resonance dip at the lowest frequency (Band I, arrow 1) is clear at all air gaps in the spectra. Its frequency is changed from 0.321 THz to 0.38 THz when the air gap

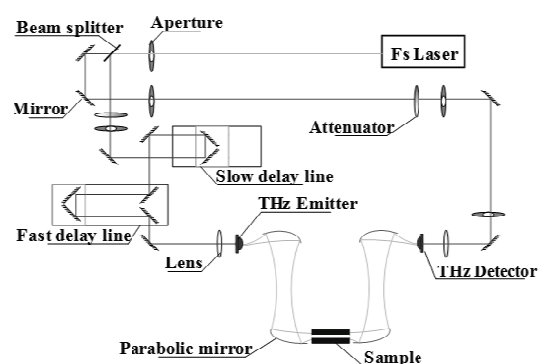
decreases from $880\ \mu\text{m}$ to $510\ \mu\text{m}$, respectively. Interestingly, the resonance dip at high frequency (Band II, arrow 2) in the spectrum exists explicitly at certain air gap from $510\ \mu\text{m}$ to $760\ \mu\text{m}$. The resonance dip (Band III, arrow 3) can be observable at the air gaps of $670\ \mu\text{m}$, $620\ \mu\text{m}$, $585\ \mu\text{m}$, $555\ \mu\text{m}$, and $510\ \mu\text{m}$, respectively. The dramatic decrease for the three bands comes from the increasing loss induced by more abrupt junctions between the waveguide sections, and the following small change is owing to the high energy concentration in the deep cavity. In Fig. 5, the two dimensional transmission map is obtained by varying incident frequency f and air gap l/d .



(a)



(b)



(c)

Fig. 1. Experimental structure and setup: (a) structure sketch of cavity (cavities) waveguide resonant structure, (b) schematic of PPWG sample, and (c) THz-TDS system.

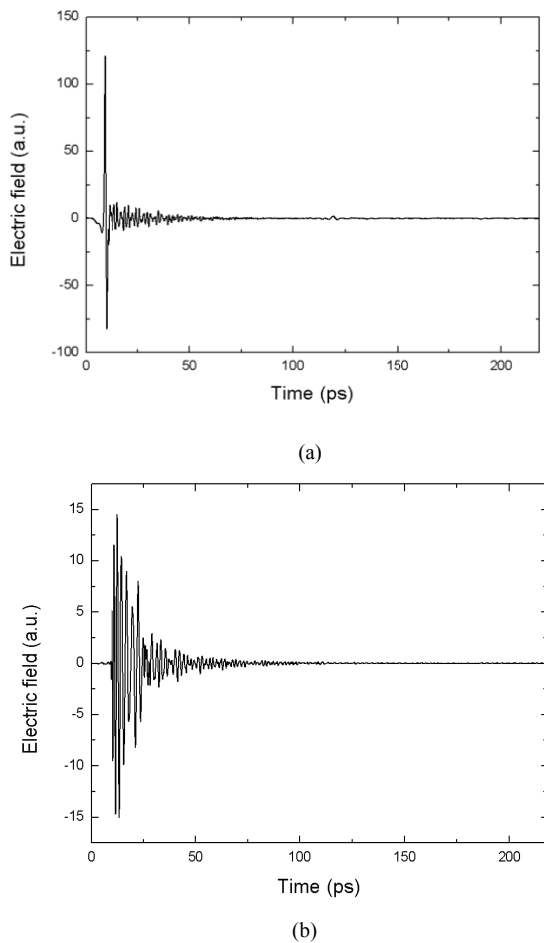


Fig. 2. Time scans corresponding to THz wave propagation through: (a) free space and (b) PPWG with $h_1=0 \mu\text{m}$, $h_2=1400 \mu\text{m}$, and $d=555 \mu\text{m}$.

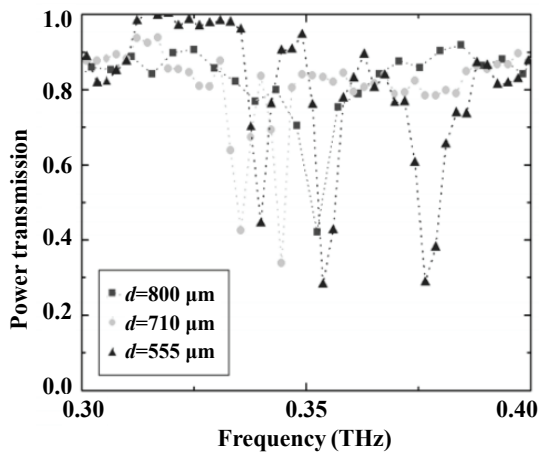


Fig. 3. Measured power transmission spectra of grooved waveguide with $h_1=0 \mu\text{m}$ and $h_2=1400 \mu\text{m}$ but varying d .

Finally, we make a simple comparison of our proposed structure with some similar structures in the THz region^{[10],[12]}. Since the single groove structure inside the waveguide corresponds to the resonant features in the transmission spectra, our structure can operate as a multiband notch filter by using the single deep cavity,

which is very different from the single band notch filter based on one shallow grooved TE-mode PPWG ($h_1=0 \mu\text{m}$, $h_2=412 \mu\text{m}$, $w=460 \mu\text{m}$) in [12]. Compared with the TEM mode PPWG structure in [10], the multiple resonances are due to the excitation of high order cavity modes. Most importantly, for the small air gap, the novel phenomena of resonance frequency deviation and high order cavity modes have been both numerically and experimentally verified in this paper.

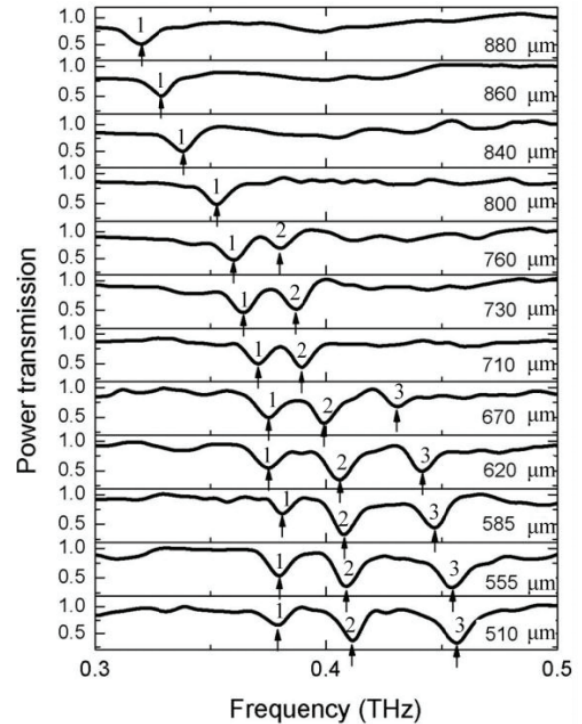


Fig. 4. Power transmission spectra for different air gap d . The arrows indicate sharp resonance dip (arrow 1: Band I; arrow 2: Band II; arrow 3: Band III).

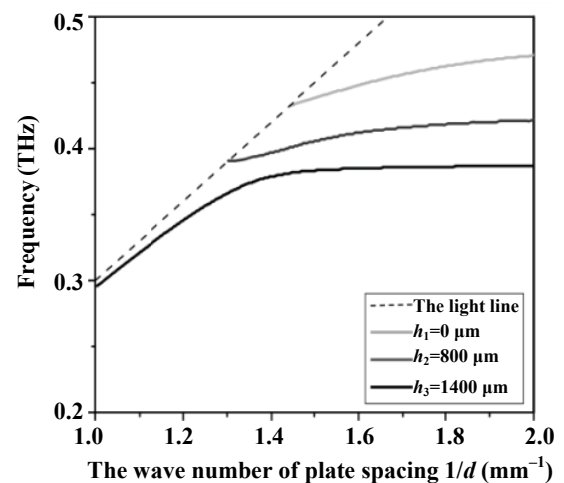


Fig. 5. Simulated transmission map as a function of $1/d$ with $h_1=0 \mu\text{m}$, $h_2=800 \mu\text{m}$, and $h_3=1400 \mu\text{m}$.

Besides, a multiband THz notch filter with band number control can be realized by tuning the air gap. Note

that the depth h_2 ($h_1=0\ \mu\text{m}$, $L=0\ \mu\text{m}$) can also be deeper to excite higher order cavity modes, making the deep grooved waveguide potentially a very effective notch filter to achieve much more bands control.

3. PPWG with Double Cavities

The PPWG-cavities system introduces the waveguide spacing as another degree of freedom. By mechanically tuning the waveguide spacing between the two plates, we experimentally demonstrate the control of THz waves in the PPWG-cavities system with the appropriate fixed shifting length between the two cavities that can achieve EIT.

The PPWG-cavities system consists of two aluminum plates, each with a micro-machined rectangular cavity, as shown in Fig. 1 (b). All cavities have the identical geometry with a width of $w=470\ \mu\text{m}$ ($\pm 5\ \mu\text{m}$) and a depth of $h_1=h_2=420\ \mu\text{m}$ ($\pm 5\ \mu\text{m}$). We fabricated four sets of PPWG cavities configurations: a perfect symmetric one with the top and the bottom cavities exactly at the center of the waveguide and asymmetric configurations made by keeping the top cavity fixed and displacing the bottom cavity from the center position with $L=0\ \mu\text{m}$, $100\ \mu\text{m}$, $200\ \mu\text{m}$, and $300\ \mu\text{m}$, respectively, where L represents the bottom cavity shifting length from the center in the propagation direction and d represents the length of the plates. A combined fast and slow scan-based THz time domain spectroscopy (THz-TDS) was used for evaluating the transmission properties of the PPWG system. The fast optical delay line with a 110 ps range can be obtained. If we combine it with the slow scan, the overall delay line can be expanded to 218.4 ps. This means the experimental spectra resolution can reach 4.58 GHz. The electric field of the incident beam was oriented parallelly to the plates in order to excite the TE mode.

From the simulation of the electric field distribution, the mode of the low frequency transmission dip should be the inverse phase coupling of the double cavities in Fig. 6 (a), and the high frequency should be the phase coupling in Fig. 6 (b).

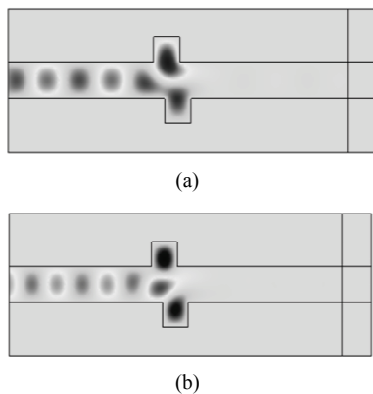


Fig. 6. Electric field distribution of transmission dip's center frequency: (a) low frequency and (b) high frequency.

Fig. 7 shows the measured transmission spectra of the PPWG, the PPWG with a single cavity ($d=650\ \mu\text{m}$) and two cavities ($d=650\ \mu\text{m}$, $L=200\ \mu\text{m}$), respectively. The PPWG without any cavity acts as the reference. The entire loss is exhibited in each picture of Fig. 8 when the frequency of the incident wave is lower than the cutoff frequency $f_c=c/2d=0.23\ \text{THz}$ ^{[11],[26]}. For the single-cavity structured PPWG, there was a resonant frequency at 0.381 THz. When we added another cavity on the bottom plate and set the staggered length $L=200\ \mu\text{m}$, two resonant dips appeared at 0.354 THz and 0.41 THz, respectively. The water-vapor absorption at 0.557 THz and 0.752 THz could also be observed in this range, which cannot affect our experimental results.

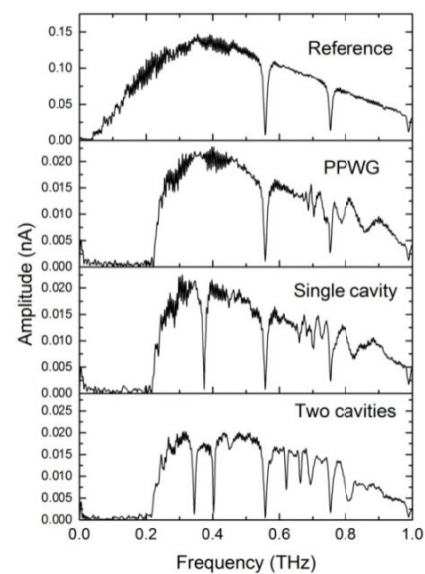


Fig. 7. Transmission spectra of the THz wave transmitted through the PPWG with spacing $d=650\ \mu\text{m}$, single cavity ($w=470\ \mu\text{m}$, $h=420\ \mu\text{m}$), and two cavities with the shifted length $L=200\ \mu\text{m}$.

Next, we discuss the influence of the shifting length L on the transmission response. For this discussion, the length of the top and bottom plates was fixed at $d=650\ \mu\text{m}$. The PPWG without any cavity acted as the reference. Fig. 8 shows the power transmission of the PPWG-cavities system with different L . For the structure with symmetry ($L=0\ \mu\text{m}$), only one broad symmetric resonant dip at 0.417 THz was observed. For the PPWG cavities structure with $L=100\ \mu\text{m}$, asymmetry was introduced, resulting in a new resonant dip at a lower frequency (0.354 THz). When the bottom cavity was further shifted up to $L=200\ \mu\text{m}$, the lower resonant frequency showed blue-shift and the high resonant frequency showed red-shift. A transparent band between the two resonant dips becomes narrow as well as the decrease of the transmittance. We observed an EIT-like transmission which was similar to previous investigations for meta-material and plasmon analogues of EIT. For the asymmetric structure with $L=300\ \mu\text{m}$, two resonance dips came closer and the transmission peak reduced further. The

experimental results agree well with the numerical results in Fig. 8 and the deviation is probably caused by the fabrication imperfections of the sample, which introduce further asymmetry and rearrangement of some resonant frequencies. For a complete picture of resonant frequencies change, several calculations were performed with the variation of the shifting length from 0 μm to 450 μm . The detuning $|\omega_1 - \omega_2|$ (ω_1 and ω_2 are low and high resonant frequencies, respectively) decreases and the transparency window narrows down with the increase of the shifting length L .

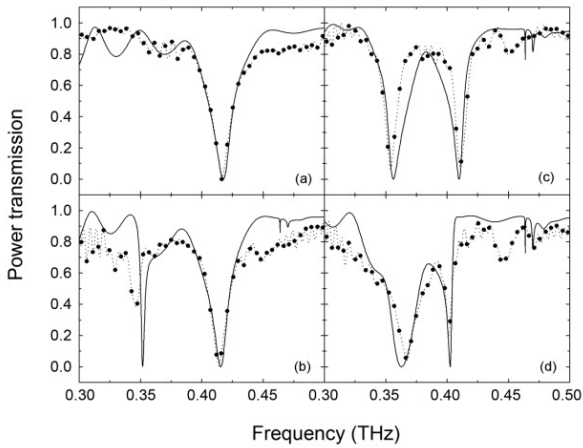


Fig. 8. Fourier-transformed intensity of the THz wave forms with different L (solid line: simulated, dash line & dots: experimental): (a) $L=0 \mu\text{m}$, (b) $L=100 \mu\text{m}$, (c) $L=200 \mu\text{m}$, and (d) $L=300 \mu\text{m}$.

This EIT-like transmission can also be explained by analogy to the coupling of bright modes and dark modes. When the bottom cavity is set symmetrically to the top one, only one resonant dip, which corresponds to the two bright modes (each of them has the same resonant frequency), can be excited in both cavities simultaneously. In this condition, the dark modes cannot be excited. When the bottom cavity is shifted backward from the symmetric position, due to the identical geometry of the two cavities, the incident wave first arrives at the top cavity and couples with it. The shifted bottom cavity can hardly be interacted directly with the incident wave any more but can couple with the top cavity. In other words, the top cavity acts as the “radiative” resonator (a bright mode) that is coupled to a “bus” waveguide; the bottom cavity acts as the “sub-radiant” resonator (a quasi-dark mode, induced by the shifting length of two cavities) that cannot be coupled to the “bus” waveguide. This physical picture is similar to the unit cell (consists of an upper gold strip as a bright mode, a pair of lower gold strips as a dark mode, and a dielectric spacer) Then this EIT-like transmission can also be seen as the coupling between bright modes and quasi-dark modes when the symmetry is broken.

Besides, the influence of the length of the top and bottom plates d was also investigated^[20]. Four different

waveguide spacings with $d=610 \mu\text{m}$, $670 \mu\text{m}$, $740 \mu\text{m}$, and $780 \mu\text{m}$, were used to study the characteristics of the EIT. Fig. 9 shows the experimental (dots) and simulation (black lines) power transmissions by comparing the spectra of the propagated pulses with and without the cavities. The metal is set as a perfect electrical conductor in the simulation due to the disregard for the attenuation loss of the metal in the THz range. At least three more observations may be inferred by looking at Fig. 9: i) Fig. 9 exhibits a complete loss of spectral power up to the cutoff frequencies of 0.244 THz, 0.236 THz, 0.202 THz, and 0.192 THz, corresponding to $d=610 \mu\text{m}$, $670 \mu\text{m}$, $740 \mu\text{m}$, and $780 \mu\text{m}$, respectively. ii) The transmission shows strong EIT effect, when d is increased from 610 μm to 780 μm , the low asymmetric resonances shows red-shift. The asymmetric resonant frequencies for $d=610 \mu\text{m}$, $670 \mu\text{m}$, $740 \mu\text{m}$, and $780 \mu\text{m}$ are 0.395 THz, 0.379 THz, 0.354 THz, and 0.338 THz, respectively. This red-shift of high symmetric resonances can also be found for $d=610 \mu\text{m}$ and $670 \mu\text{m}$, where the resonant frequencies are 0.456 THz and 0.446 THz, respectively. iii) As d is increased to 740 μm , the main symmetric resonances is degenerated in Fig.9 (c). This effect can also be found when d is equal to 780 μm . The measured and simulated results show good agreements. The deviation of experimental and numerical results is probably caused by the imperfections in the fabrication in real structures, which introduces further rearrangement of resonant frequencies.

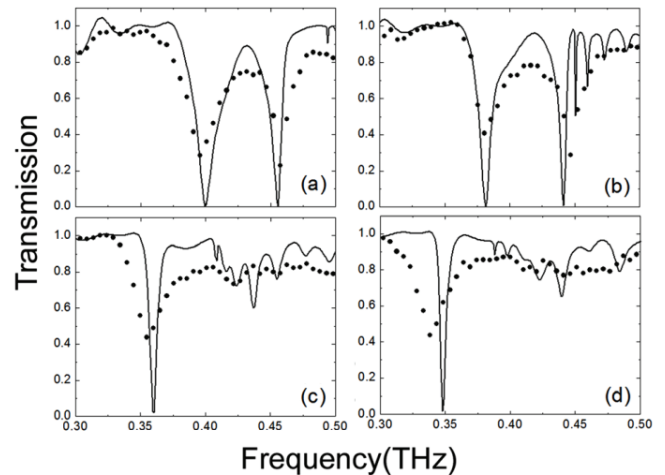


Fig. 9. Measured THz spectra with various air gaps (solid line: simulated, dots: experimental): (a) $d=610 \mu\text{m}$, (b) $d=670 \mu\text{m}$, (c) $d=740 \mu\text{m}$, and (d) $d=780 \mu\text{m}$.

Firstly, as mentioned above in the experiment, when the waveguide spacing d decreases ($1/d$ increases), the resonant frequencies of both symmetric and asymmetric resonances show red-shift. This red-shift effect is similar to the result of the PPWG with a single cavity for both TE^[12] and TM^[10] polarizations. The resonant frequency can be expressed as^[10]

$$v(d) \propto \frac{c}{2 \times (2h_{\text{eff}} + d)} \quad (1)$$

where c is the light velocity in vacuum (3×10^8 m/s= 0.3 THz/mm⁻¹) and h_{eff} is the effective cavity height. The value of h_{eff} for the asymmetric resonances is not equal to that for the symmetric resonances due to the electric field difference between two resonances at resonant frequencies (shown in Figs. 4 (b) and (d) of [17]). This process causes the red-shift of EIT peaks observed in both experiment and simulation. The mechanism of red-shift by the PPWG with two cavities is identical to that of the single cavity^[12], the only difference is that the single Fabbri-Palo (FP) resonance is supported by PPWG with one cavity and two FP resonances are supported by asymmetric PPWG cavities.

According to the relationship between the size d and λ , the dispersion diagram can be divided into three regions as in Fig. 10.

1) Region I: $d < \lambda/2$, the maximum mode order that can be excited is 0. No stable mode exists.

2) Region II: $\lambda/2 < d < \lambda$, the maximum mode order which can be excited is 1. Only the lowest order transverse electric mode TE is excited, we can observe the transmission dip in the region II.

3) Region III: $d > \lambda$, the maximum mode order is larger than 1. The lowest order transverse electric mode and higher transverse electric mode can be excited. Considering the residual effect of the transmission dip, we can observe the claw type structure in region III.

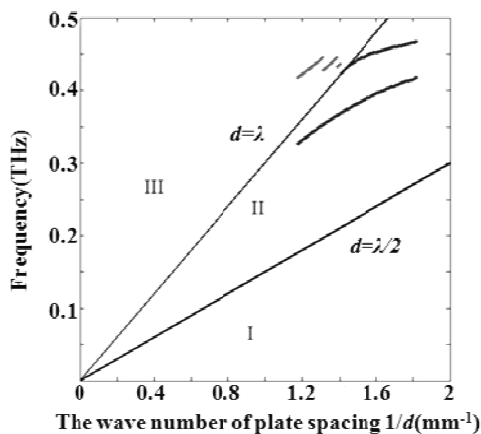


Fig. 10. Observation range of PPWG.

So far, we can describe the mechanism of manipulation of EIT in a PPWG cavities system. By fixing appropriate shifting length L (200 μm), as d increases and the two FP resonant wavelengths are larger than d (below the light line), EIT can be found obviously and the two resonances (including the transparent peak) show red-shift. Once the symmetric FP resonant wavelength is less than d , the TEM wave propagates along a “zigzag line” and acts as guided

wave. The cavities produce little influence on the transmission (that is, the FP resonances cannot exist in the region above the light line). Here the increase of d converts the FP resonances into the guided wave. Since the EIT transparent peak between two resonances comes from the destructive interference of symmetric and asymmetric resonances^[17], as the transition of symmetric FP resonances take place, this interference is broken and an on-to-off EIT peak modulation can be completed in this process. The mechanism of above manipulation is different from control of EIT in meta-material and plasmonics^{[27]–[30]}.

4. Conclusions

In conclusion, a tunable multiband terahertz notch filter is presented experimentally and numerically based on PPWG with a single deep cavity and double cavities, respectively. The adjustable air gap has been investigated to flexibly modify the filtering characteristics of the presented filter. The air gap can also be varied in the applying to adjust the band number. Because the air gap can be easily tunable by mechanical control or electrical adjustment, this deep cavity PPWG structure has great potential applications in THz communications. An on-to-off control of the EIT resonances is achieved by mechanically tuning the spacing. It may inspire interest in developing mechanically tunable waveguide based EIT, resulting in a wide range of novel compact THz devices, such as slow light components, sensitive sensors, and electromagnetically induced absorbers.

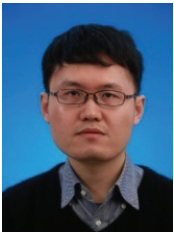
Acknowledgment

This work was supported by the Shanghai Rising-Star Program under Grant No. 14QA1403100, Program of Shanghai Subject Chief Scientist under Grant No. 14XD1403000, Hujiang Foundation of China under Grant No. C14002, Zhejiang Key Discipline of Instrument Science and Technology under Grant No. JL150505, and the New Century Excellent Talents Project from the Ministry of Education under Grant No. NCET-12-1052.

References

- [1] R. Mendis and D. Grischkowsky, “Undistorted guided-wave propagation of subpicosecond terahertz pulses,” *Optics Letter*, vol. 26, no. 11, pp. 846–848, 2001.
- [2] J. M. Nagel, P. H. Bolivar, and H. Kurz, “Modular parallel-plate THz components for cost-efficient biosensing systems,” *Semiconductor Science and Technology*, vol. 20, no. 7, pp. S281–S285, 2005.
- [3] C.-Y. Lin, M. Wu, J. A. Bloom, I. J. Cox, and M. Miller, “Rotation, scale, and translation resilient public watermarking for images,” *IEEE Trans. on Image Processing*, vol. 10, no. 5, pp. 767–782, 2001.
- [4] J. Kitagawa, M. Kodama, S. Koya, Y. Nishifuji, D. Armand, and Y. Kadoya, “THz wave propagation in two-dimensional metallic photonic crystal with mechanically tunable

- photonic-bands,” *Optics Express*, vol. 20, no. 16, pp. 17271–17280, 2012.
- [5] R. Mendis, V. Astley, J. Liu, and D. M. Mittleman, “Terahertz microfluidic sensor based on a parallel-plate waveguide resonant cavity,” *Applied Physics Letter*, vol. 95, no. 17, pp. 171113-1–171113-3, 2009.
- [6] E. S. Lee, J.-K. So, G.-S. Park, D. Kim, C.-S. Kee, and T. I. Jeon, “Terahertz band gaps induced by metal grooves inside parallel-plate waveguides,” *Optics Express*, vol. 20, no. 6, pp. 6116–6123, 2012.
- [7] E. S. Lee, S.-G. Lee, C.-S. Kee, and T.-I. Jeon, “Terahertz notch and low-pass filters based on band gaps properties by using metal slits in tapered parallel-plate waveguides,” *Optics Express*, vol. 19, no. 16, pp. 14852–14859, 2011.
- [8] L. Chen, C.-M. Gao, J.-M. Xu, X.-F. Zang, B. Cao, and Y.-M. Zhu, “Observation of electromagnetically induced transparency-like transmission in terahertz asymmetric waveguide-cavities systems,” *Optics Letter*, vol. 38, no. 9, pp. 1379–1381, 2013.
- [9] V. Astley, K. S. Reichel, J. Jones, R. Mendis, and D. M. Mittleman, “Terahertz multichannel microfluidic sensor based on parallel-plate waveguide resonant cavities,” *Applied Physics Letter*, vol. 100, no. 23, pp. 231108-1–231108-4, 2012.
- [10] E. S. Lee and T. Jeon, “Tunable THz notch filter with a single groove inside parallel-plate waveguides,” *Optics Express*, vol. 20, no. 28, pp. 29605–29612, 2012.
- [11] R. Mendis and D. M. Mittleman, “Comparison of the lowest-order transverse-electric (TE) and transverse-magnetic (TEM) modes of the parallel-plate waveguide for terahertz pulse applications,” *Optics Express*, vol. 17, no. 17, pp. 14839–14850, 2009.
- [12] V. Astley, B. McCracken, R. Mendis, and D. M. Mittleman, “Analysis of rectangular resonant cavities in terahertz parallel-plate waveguides,” *Optics Letter*, vol. 36, no. 8, pp. 1452–1454, 2011.
- [13] L. Chen, Z.-Q. Cao, F. Ou, H.-G. Li, Q.-S. Shen, and H.-C. Qiao, “Observation of large positive and negative lateral shifts of a reflected beam from symmetrical metal-cladding waveguides,” *Optics Letter*, vol. 32, no. 11, pp. 1432–1434, 2007.
- [14] X.-S. Lin and X.-G. Huang, “Tooth-shaped plasmonic waveguide filters with nanometric sizes,” *Optics Letter*, vol. 33, no. 23, pp. 2874–2876, 2008.
- [15] M. Yosuke, O. Toshihiro, H. Masanobu, F. Masuo, and N. Masatoshi, “Characteristics of gap plasmon waveguide with stub structures,” *Optics Express*, vol. 16, no. 12, pp. 16314–16325, 2008.
- [16] X. Piao, S. Yu, S. Koo, K. Lee, and N. Park, “Fano-type spectral asymmetry and its control for plasmonic metal-insulator-metal stub structures,” *Optics Express*, vol. 19, no. 11, pp. 10907–10912, 2011.
- [17] L. Chen, C.-M. Gao, J.-M. Xu, X.-F. Zang, B. Cai, and Y.-M. Zhu, “Observation of electromagnetically induced transparency-like transmission in terahertz asymmetric waveguide-cavities systems,” *Optics Letter*, vol. 38, no. 9, pp. 1379–1381, 2013.
- [18] X.-F. Zang, T. Zhou, B. Cai, and Y.-M. Zhu, “Single-photon transport properties in an optical waveguide coupled with a Λ -type three-level atom,” *Journal of the Optical Society of American B*, vol. 30, no. 5, pp. 1135–1140, 2013.
- [19] X.-F. Zang, T. Zhou, B. Cai, and Y.-M. Zhu, “Controlling single-photon transport properties in a waveguide coupled with two separated atoms,” *Journal of Physics B*, vol. 46, no. 14, pp. 145504-1–145504-6, 2013.
- [20] L. Chen, J.-M. Xu, C.-M. Gao, X.-F. Zang, B. Cai, and Y.-M. Zhu, “Manipulating terahertz electromagnetic induced transparency through parallel plate waveguide cavities,” *Applied Physics Letters*, vol. 103, no. 25, pp. 251105-1–251105-4, 2013.
- [21] Y.-M. Zhu, T. Unuma, K. Shibata, and K. Hirakawa, “Femtosecond acceleration of electrons under very high electric fields in bulk GaAs investigated by time-domain terahertz spectroscopy,” *Applied Physics Letters*, vol. 93, no. 4, pp. 042116, 2008.
- [22] Y.-M. Zhu, T. Unuma, K. Shibata, and K. Hirakawa, “Power dissipation spectra and terahertz intervalley transfer gain in bulk GaAs under high electric fields,” *Applied Physics Letters*, vol. 93, no. 23, pp. 232102-1–232102-3, 2008.
- [23] Y.-M. Zhu, L. Chen, Y. Peng, M.-H. Yuan, Y. Wen, and S.-L. Zhuang, “Temperature dependence of nonequilibrium transport time of electrons in bulk GaAs investigated by time-domain terahertz spectroscopy,” *Applied Physics Letters*, vol. 99, no. 2, pp. 022111-1–022111-3, 2011.
- [24] Y.-M. Zhu and S.-L. Zhuang, “Terahertz electromagnetic waves emit from semiconductor investigated by time domain terahertz spectroscopy,” *Chinese Optics Letters*, vol. 9, no. 11, pp. 110007, 2011.
- [25] J.-M. Xu, L. Chen, L. Xie, S.-Q. Du, M.-H. Yuan, Y. Peng, and Y.-M. Zhu, “Effect of boundary condition and periodical extension on transmission characteristics of terahertz filters with periodical hole array structure fabricated on aluminum slab,” *Plasmonics*, vol. 8, no. 3, pp. 1293–1297, 2013.
- [26] R. Mendis, V. Astley, J. Liu, and D. M. Mittleman, “Terahertz microfluidic sensor based on a parallel-plate waveguide resonant cavity,” *Applied Physics Letters*, vol. 95, no. 17, pp. 171113-1–171113-3, 2009.
- [27] Y. Huang, C.-J. Min, and G. Veronis, “Subwavelength slow-light waveguides based on a plasmonic analogue of electromagnetically induced transparency,” *Applied Physics Letters*, vol. 99, no. 14, pp. 143117-1–143117-3, 2011.
- [28] Z.-H. Han and S. I. Bozhevolnyi, “Plasmon-induced transparency with detuned ultracompact Fabry-Perot resonators in integrated plasmonic devices,” *Optics Express*, vol. 19, no. 4, pp. 3251–3257, 2011.
- [29] Z.-Y. Li, Y.-F. Ma, R. Huang, R. J. Singh, J.-Q. Gu, Z. Tian, J.-G. Han, and W.-L. Zhang, “Manipulating the plasmon-induced transparency in terahertz metamaterials,” *Optics Express*, vol. 19, no. 9, pp. 8912–8919, 2011.
- [30] J.-Q. Gu, R. Singh, X.-J. Liu, X.-Q. Zhang, Y.-F. Ma, S. Zhang, S. A. Maier, Z. Tian, A. K. Azad, H.-T. Chen, A. J. Taylor, J.-G. Han, and W.-L. Zhang, “Active control of electromagnetically induced transparency analogue in terahertz metamaterials,” *Nature Communications*, vol. 3, 1151-1–1151-6, 2012.



Lin Chen was born in Jiangsu, China in 1980. He received the B.S. and M.S. degrees from the Southeast University in 2002 and 2005, both in electrical engineering, and the Ph.D. degree from the Shanghai Jiao Tong University in 2008, in optics, respectively. Now he is an associate professor with the University of Shanghai for Science and

Technology. His research interests include terahertz waveguide, meta-material, and lab on chip. He has been awarded the “Chen Guang” Scholar in 2009, China Instrument Society-JinGuofan Youth Award in 2011, and Shanghai “rising star” Scholar in 2014. He has published more than 40 SCI papers and 20 patents. As the project leader, he is also responsible for several national funds and funds supported by Shanghai government.



Dan-Ni Wang was born in Anhui, China in 1991. She received her B.S. degree from the Shanghai Normal University in 2013. She won the National Scholarship and Shuikang Feng Scholarship in 2012. She was awarded the outstanding graduates of Shanghai in 2013. Now, she is a postgraduate with the University of Shanghai for Science and Technology. Her

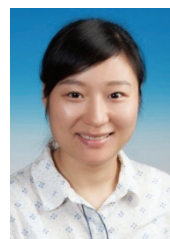
research interests include terahertz waveguide, meta-material, and sensor chip.



Yi-Ming Zhu graduated from the University of Tokyo, now he is a professor with the University of Shanghai for Science and Technology, the vice director of the Shanghai Key Lab of Modern Optical System, and the associate dean of the Research Institute of Optoelectronics. He studied at Shanghai

Jiaotong University from 1998 to 2002 and received a bachelor degree in apply physics. In 2003, he began to

work as an assistant researcher with the Research Center for Advanced Science and Technology, University of Tokyo. He won the Japanese Government Scholarship in 2004 and studied electronics engineering in University of Tokyo as a doctor candidate. He gained his Ph.D. degree in electronics engineering in 2008. He has published more than 100 papers on SCI/EI journals as the first author or corresponding author, including two publication on Nature Group series, more than 20 papers in SCI section II and above, He has also presided more than 20 projects at the national and ministerial/provincial levels, which include one project supported by National 863 Project, 3 projects supported by National Natural Science Foundation of China, 2 sub-projects supported by National 973 Project, 2 projects supported by Major National Development Project of Scientific Instrument and Equipment, etc.



Yan Peng was born in Anhui, China in 1982. She received the B.S. degree from the Anhui Normal University in 2004 and the Ph.D. degree from the East China Normal University in 2009, both in physics. She is an associate professor with the University of Shanghai for Science and Technology. Her research interests include ultrafast optics, terahertz, high-order

harmonic generation, and microstructure.

As a project leader, Dr. Peng is responsible for the National Program on Key Basic Research Project of China (973 Program, sub-project), two National Development Projects of Scientific Instrument and Equipment, one National Natural Science Foundation of China, one State Scholarship Fund, and two projects from Shanghai Municipal Education Commission. She was awarded the “Chen Guang” Scholar in 2012, China Instrument Society-Jin Guofan Youth Award, and “Excellent Woman” Award of University of Shanghai for Science and Technology. Up to now, she has published more than 30 SCI papers and 20 patents.